

Exclusion of heavy, broad resonances from precise measurements of WZ and VH final states at the LHC

You-Ying Li¹, Rosy Nicolaidou², Stathes Paganis^{a,1}

¹ Department of Physics, National Taiwan University, No 1, Sec 4, Roosevelt Road, Taipei 10617, Taiwan

² IRFU, CEA, Universite Paris-Saclay, Gif-sur-Yvette; France

Received: date / Accepted: date

Abstract A novel search for heavy vector resonances in the $H \rightarrow b\bar{b}$ and $Z \rightarrow b\bar{b}$ final states in association with a leptonically decaying V (Z or W) and W -only respectively, is proposed. It is argued that excesses with respect to the Standard Model prediction should be observed in all final states (0, 1 or 2 leptons), with the 1-lepton final state being the strongest. Since the relative strengths of these excesses depend on branching ratios and efficiencies, this is a clear signal for the presence of heavy resonances or their low mass tails. A general vector-triplet model is used to explore the discovery potential as a function of the resonance mass and width. Recent Higgs to $b\bar{b}$ observation data reported by the experiments ATLAS and CMS are used to test the model. Current limits are extended to resonance widths over mass as large as 9%.

Keywords Computational methods and analysis tools, Hadron and lepton collider physics

PACS 29.85.FjData analysis · 14.80.BnStandard-model Higgs bosons

1 Introduction

Heavy vector resonances naturally appear in several extensions of the Standard Model (SM), such as GUT theories [1–3], composite Higgs [4, 5], little Higgs [6–8], and models with vector Z' [9, 10], and W' models [11]. The LHC experiments, in most cases, have performed direct searches for heavy narrow resonances decaying to dibosons and VH final states and have put limits to masses up to about 5.5 TeV [12–23].

Broader resonances ($\Gamma/m > 4\%$) appear for larger values of the resonance coupling strength to weak bosons

and the Higgs, g_V , and depending on their mass, width, and production cross section, the LHC experiments can be sensitive to a large part of the resonance distribution. It is interesting to study to what extent the experiments can be sensitive to the full distribution or tails of such resonances and what the best observables are. In this work, we start addressing this question with a specific final state: a pair of b quarks produced in association with a weak gauge boson (Z or W) that subsequently decays leptonically (where leptons ℓ are electrons and muons). The interest in this final state is because in the large coupling regime, $g_V > 3$, the heavy boson branching fraction is dominated by decays to WZ and VH , while the decays to fermions are suppressed [24]. At the same time, both the Drell-Yan $q\bar{q}$ and the VBF production modes contribute, providing non-negligible cross sections. Here, we propose as an early indirect signal of the presence of vector resonances, the simultaneous excess in the 0, 1, and 2-lepton final states, for both $WZ \rightarrow \ell\nu b\bar{b}$ and $VH \rightarrow \ell\ell(\nu)b\bar{b}$, in a measurement of the $b\bar{b}$ quark invariant mass $M_{b\bar{b}}$. The strength of these excesses in the different final states can be predicted by branching ratios and experimental efficiencies. We argue that the 0, 1, and 2-lepton final states should all be sensitive, albeit with very different sensitivity, to exotic $V' \rightarrow VH$ decays. In particular, the 1-lepton state will be the most sensitive in Higgs excesses and in addition, it should also show a smaller level of excess in the Z -boson $b\bar{b}$ peak. The pattern of these excesses should be a clear sign of a heavy vector triplet (HVT), even before its observation as a (broad) mass resonance at the TeV scale. Using a general HVT framework that is also used by the experiments to model such heavy vector triplets [25], we derive the sensitivity of a single LHC experiment as a function of the resonance width.

^astathes.paganis@cern.ch, corresponding author

In this paper, we first introduce the HVT framework and summarize the recent LHC results. In Section 3 we present an analysis used to search for heavy vector triplets at the LHC, and we report on the search potential for the $b\bar{b}+0, 1,$ and 2 -lepton final states, for a range of masses and widths. Finally, the compatibility of our predictions with the recently published 13 TeV $H \rightarrow b\bar{b}$ data from ATLAS and CMS in terms of expected and observed limits, is discussed.

2 BSM Heavy Vector Resonances

A general HVT phenomenological Lagrangian can be used for the modelling of resonances predicted by a wide range of Beyond the Standard Model (BSM) scenarios [25]. The Lagrangian describing the interactions of these resonances $V^{a'}$, $a = 1, 2, 3$ with quarks, leptons, vector bosons and the Higgs boson is shown below:

$$\mathcal{L}_V^{int} = -\frac{g^2 c_F}{g_V} V_\mu^{a'} \bar{q}_k \gamma^\mu \frac{\sigma_a}{2} q_k - \frac{g^2 c_F}{g_V} V_\mu^{a'} \bar{\ell}_k \gamma^\mu \frac{\sigma_a}{2} \ell_k - g_V c_H \left(V_\mu^{a'} H^\dagger \frac{\sigma_a}{2} i D^\mu H + \text{hc} \right),$$

where q_k and ℓ_k are the quark and lepton weak doublets, H is the Higgs doublet and σ^a the three Pauli matrices. In this Lagrangian, the HVT triplet $V^{a'} = (W^{+'}, W^{-'}, Z')$ interacts with the Higgs doublet, i.e. the longitudinal degrees of freedom of the SM W and Z bosons and the SM Higgs, with a coupling strength g_V . In order to allow for a broader class of models, this coupling strength can be varied by the parameter c_H , so in the Lagrangian the full coupling to the SM weak and Higgs bosons is $g_V c_H$. The HVT resonances also couple to the SM fermions, again through their coupling to the SM weak and Higgs bosons, g^2/g_V , where g is the SM $SU(2)_L$ weak gauge coupling. This coupling between HVT resonances and fermions is also controlled by an additional parameter c_F to allow for a broader range of models to be included, as follows: $g^2 c_F/g_V$. As discussed in [23], the experiments consider two Drell Yan (DY) production scenarios: model A is a scenario that reproduces the phenomenology of weakly coupled models based on an extended gauge symmetry [9]. In this case, the couplings are $\frac{g^2 c_F}{g_V} = -0.55$ and $g_V c_H = -0.56$, with the fermion coupling being universal. The second DY scenario, referred to as model B, implements a strongly coupled scenario as in composite Higgs models with $\frac{g^2 c_F}{g_V} = 0.14$ and $g_V c_H = -2.9$. In model B, the V' resonances are broader than in the weakly coupled scenario, model A, but for $|g_V c_H| \leq 3$ they remain narrow relative to the experimental resolution. For $|g_V c_H| > 3$, the resonance intrinsic width

becomes significant and cannot be neglected. In summary, the ATLAS and CMS benchmarks correspond for Model A to $c_H = -\frac{g^2}{g_V^2}$, $c_F = -\frac{1}{3}$ and $g_V = 1$, and for model B to $c_H = -1$, $c_F = 1$ and $g_V = 3$. ATLAS and CMS experimental data from direct m_{VH} and m_{VV} searches, exclude part of the parameter phase space (g_V, c_H, c_F) , for which the intrinsic width Γ of the new bosons is dominated by the experimental resolution ($\sim 4\%$ of the mass). This is also the case, for example, for $|g_V c_H| \leq 3$, where negligible natural width is assumed (narrow width assumption). The goal of this work is to explore the part of the HVT parameter space with $|g_V c_H| > 3$, where the heavy resonances have a significant natural width. Following the model B benchmark, we fix the two constant factors to $c_H = -1$, $c_F = 1$ and allow g_V to vary.

Results from recent experimental analyses that exclude part of the HVT phase space are shown in Fig. 1. The validity of these exclusions is actually limited due to the narrow width approximation. For larger, $|g_V c_H| > 3$, couplings, the width grows and becomes comparable to or larger than the experimental resolution, leaving a large part of the HVT phase space unexcluded: $3 < |g_V c_H| < 4\pi$, where $g_V \simeq 4\pi$ is the perturbative limit. This is true even for resonance masses of order TeV.

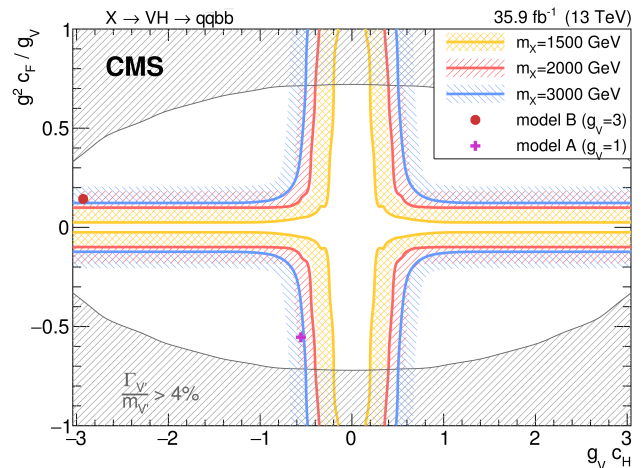


Fig. 1 CMS, [21], observed 95% CL exclusion contours in the HVT parameter space $g_V c_H, (g^2/g_V) c_F$ for narrow resonances of mass 1.5 TeV, 2.0 TeV and 3.0 TeV. Due to the narrow width approximation assumption, the exclusion validity is restricted to roughly $|g_V c_H| \leq 3$ and outside the hatched area shown, thus leaving a large part of the available phase space unconstrained ($3 < |g_V c_H| < 4\pi$). Similar limits have been published by ATLAS, [15].

In this work we argue that the presence of non-zero width resonances, could be observed as an excess of events in the $VH \rightarrow \ell\ell(\nu)\bar{b}\bar{b}$ and $WZ \rightarrow \ell\nu b\bar{b}$ decays

with 0, 1, or 2 leptons in the final state. Independent of the fact that due to the experimental resolution the close-by $Z \rightarrow b\bar{b}$ and $H \rightarrow b\bar{b}$ peaks have a partial overlap, in the 1-lepton case the excess must be present in both peaks, while in the 0 and 2-lepton final states it should appear only in the Higgs peak (Z' does not couple to ZZ). In addition, the excess in the 1-lepton category should be more significant, since in this case both W^+ and W^- contribute. A combined analysis of the three final states can quantify the excess and correlate it to events with $b\bar{b}$ pairs of higher p_T than in the SM Higgs production, since these pairs originate from heavy TeV-scale objects.

ATLAS and CMS recently published results in the search for the SM $H \rightarrow b\bar{b}$ in association with a gauge boson decaying leptonically [26, 27]. This final state is identical with the one we propose here having sensitivity to HVT resonances. Both experiments report the measured M_{bb} invariant mass as shown in Figures 2 and 3, for an integrated luminosity of $\sim 80 \text{ fb}^{-1}$ at 13 TeV.

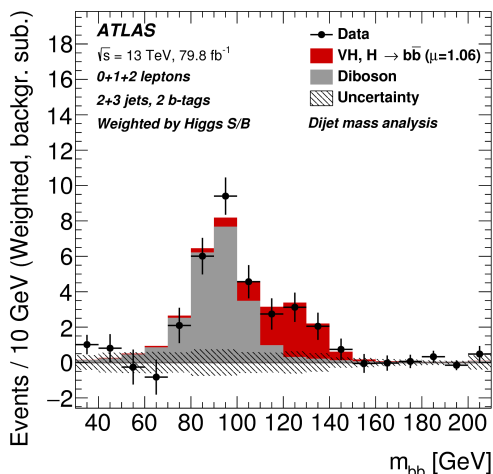


Fig. 2 Weighted bottom anti-bottom quark invariant mass data from ATLAS for 79.8 fb^{-1} [26]. The plot includes all final states with 0, 1 and 2 leptons and it compares the data yield with $1.06 \times$ the SM expectation of $H \rightarrow b\bar{b}$, and the SM expectation of $Z \rightarrow b\bar{b}$.

Broad heavy resonances mainly decaying to dibosons and pairs of fermions, occur for larger values of the g_V coupling ($g_V > 3$ for $c_H = -1$ and $c_F = 1$). The resonance width as a function of g_V is shown in Fig. 4 and the branching ratios to a pair of fermions and diboson final states are shown in Fig. 5. In both figures the calculations shown were performed by implementing the HVT model in MadGraph5 [28]. Fig. 4 shows that for $g_V > 3$ the resonance natural width over the mass ratio exceeds $\sim 3\%$, and as it can be seen in Fig. 5, the

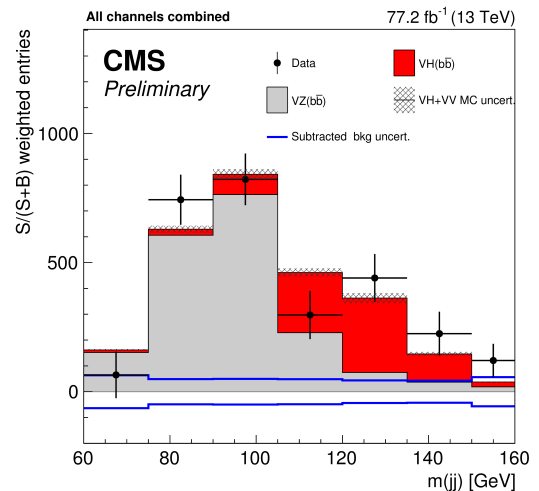


Fig. 3 Weighted bottom anti-bottom quark invariant mass data from CMS for $\sim 77.2 \text{ fb}^{-1}$ [27]. The plot includes all final states with 0, 1 and 2 leptons and it compares the data yield with the SM expectation of $H \rightarrow b\bar{b}$ and the SM expectation of $Z \rightarrow b\bar{b}$.

resonance decay to dibosons (VH , VV) is dominant. Direct searches for resonances in the VV and VH channels assume narrow resonance width that corresponds to $g_V \leq 3$, leaving unexcluded a large part of the HVT model parameter space.

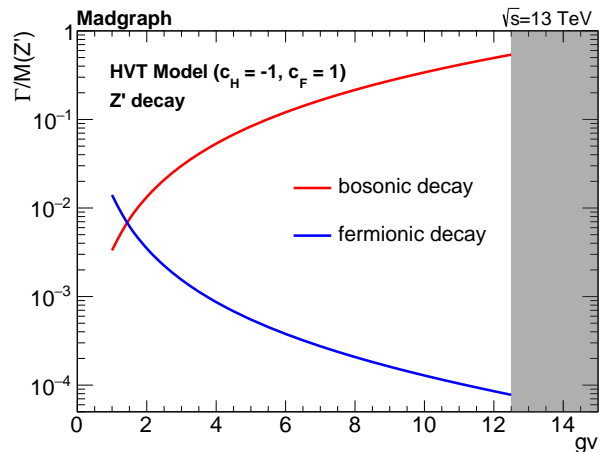


Fig. 4 Heavy resonance width for bosonic and fermionic decays as a function of the g_V coupling.

The magnitude of the impact of these resonances on SM measurements depends on their cross section which in turn, depends on the mass and the g_V coupling. Heavy resonance Drell-Yan and Vector Boson Fusion (VBF) production cross sections for masses in the range 1-3 TeV are shown in Fig. 6. The DY mode is always dominant up to large values of g_V close to the perturbative limit $g_V \simeq 4\pi$, and the total cross section drops with g_V . In Fig. 6 we can see that in the mass range

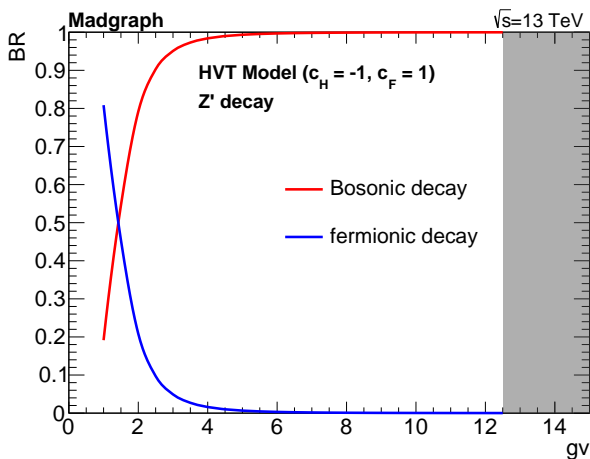


Fig. 5 Heavy resonance branching ratio to bosonic and fermionic decays as a function of the g_V coupling.

1–2 TeV, the cross sections for $g_V > 3$ range from $O(1)$ to $O(100)$ fb, leading to non-vanishing contributions at present and future measurements. For parts of the parameter space corresponding to low resonance masses and high g_V that are theoretically excluded (parts for which the input electroweak parameters α_{EW} , G_F and M_Z , are not reproduced by the HVT model), the cross section is not provided in Fig. 6.

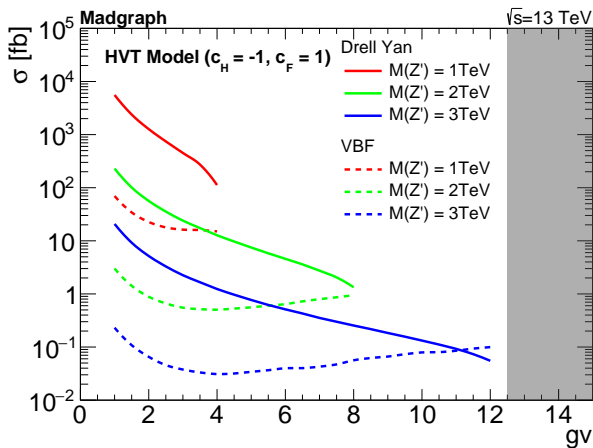


Fig. 6 Heavy resonance cross sections for the DY and VBF production modes, as a function of the g_V coupling.

3 Resonance Search Potential at Colliders

To evaluate the expected signal yields for a broad range of masses and widths, we rely on Monte Carlo samples generated with MadGraph5, [28], interfaced to PYTHIA [29]. To simulate the response of an LHC-like experiment, realistic resolution and reconstruction efficiencies for electrons, muons, photons and jets were ap-

plied with the Delphes framework [30]. The specific cut-based event selection was based on the recent VH with $H \rightarrow b\bar{b}$ results from ATLAS and CMS [26, 27]. As discussed later, the efficiencies were normalized to the experimental ones. The selected events were split in three categories according to the final state: two b jets with 0, 1 or 2 leptons. We follow more closely the ATLAS selection including the requirement of 2 or more jets out of which exactly two must be b jets. We will call this SM selection, the baseline selection, in order to differentiate from additional discriminants which enhance the BSM Higgs signal. The BSM Higgs signal decays to a $b\bar{b}$ pair with a transverse momentum, p_\perp , significantly larger than the SM Higgs. For this reason, an additional requirement applied to the baseline analysis, is a cut on the transverse momentum of the $b\bar{b}$ system. As in the LHC analyses, we only consider resolved $b\bar{b}$ pairs although the search can be extended to a single, fat $b\bar{b}$ jet analysis. As a discriminant, the $b\bar{b}$ invariant mass M_{bb} is used, which after full selection and subtraction of the $b\bar{b}$ continuum shows two peaks due to the presence of $Z \rightarrow b\bar{b}$ and $H \rightarrow b\bar{b}$.

The characteristic of the BSM signal is that the non-SM produced $H \rightarrow b\bar{b}$ has high p_\perp . This can be seen in Fig. 7, where the exotic Higgs has typical $p_\perp > 150$ GeV while the SM Higgs is softer. The expected

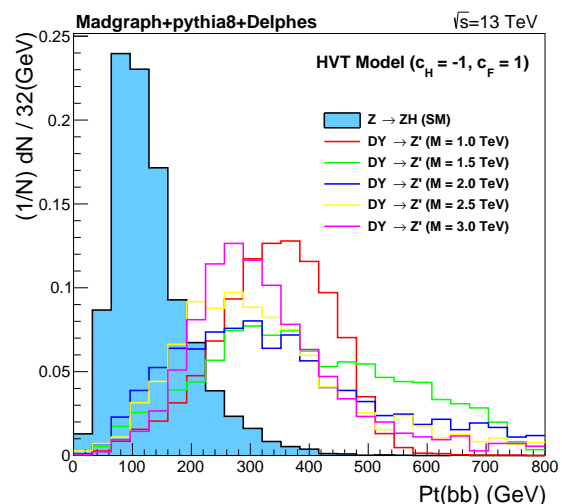


Fig. 7 Exotic Higgs $\rightarrow b\bar{b}$ transverse momentum, p_\perp , originating from heavy vector resonances, compared with SM Higgs p_\perp . Exotic Higgs bosons are typically of higher p_\perp ($p_\perp > 150$ GeV).

signal and resonant SM background yields for the baseline selection are presented in Table 1 for the 0, 1 and 2-lepton final states, for a resonance of mass 1.5 TeV, $g_V = 5$ and an integrated luminosity of 100 fb^{-1} . For a $p_\perp > 200$ GeV cut, we observe a significant increase

Process $qq \rightarrow V'$	$\sigma \times BR$ [fb]	$A \times \epsilon$ [%]	Yield [100fb ⁻¹]	Yield $p_{\perp} >$ 200 GeV
$Z' \rightarrow ZH \rightarrow \nu\nu b\bar{b}$	1.58	2.45	3.78	3.51
$Z \rightarrow ZH \rightarrow \nu\nu b\bar{b}$	97.2	5.01	486	224
$ZZ \rightarrow \nu\nu jj$	2580	0.27	697	248
$W' \rightarrow WH \rightarrow \ell\nu b\bar{b}$	3.87	5.5	21.3	19.4
$W' \rightarrow WZ \rightarrow \ell\nu jj$	3.79	0.23	0.81	0.59
$W \rightarrow WH \rightarrow \ell\nu b\bar{b}$	225	1.44	324	148
$WZ \rightarrow \ell\nu jj$	4148	0.13	529	173
$Z' \rightarrow ZH \rightarrow \ell\ell b\bar{b}$	0.553	4.76	2.6	2.2
$Z \rightarrow ZH \rightarrow \ell\ell b\bar{b}$	34.2	13.7	467	68.6
$ZZ \rightarrow \ell\ell jj$	910	0.96	875	72.6

Table 1 Signal yield and resonant SM background yields for a 1.5 TeV resonance, $g_V = 5$ and an integrated luminosity of 100 fb⁻¹, after baseline selection, and after an additional $p_{\perp} > 200$ GeV cut (last column). The resonance width over its mass is $\Gamma/m \simeq 10\%$.

in the fraction of BSM signal over the SM resonant yields, that allows to estimate the discovery potential as a function of the HVT model parameters. In the calculations shown in Table 1, in order to realistically estimate the heavy resonance parameter space that can be probed at LHC as a function of luminosity, we have normalized the efficiencies to the published results by the LHC experiments. In this way, we maintain realistic non-resonant background levels and to some extent take systematic differences between the full simulation used by the experiments and the fast simulation used here partially into account. The signal efficiency \times acceptance is at the level of few % and based on the signal cross-section expectations summarized in Fig. 6, observable excesses in M_{bb} should be expected for broad resonance masses below 2 TeV, even for present LHC luminosities.

Example scenarios with parameters $M_{Z'} = 1.5$ TeV, $g_V = 4$ and $g_V = 5$ after baseline selection and a tight transverse momentum cut $p_{\perp} > 300$ GeV, for which the bosonic decay branching ratio is dominant, are presented in Figures 8 and 9 respectively. In these Figures, the combined M_{bb} distribution is shown for an integrated luminosity of 200 fb⁻¹. Assuming that the new physics does not modify significantly the SM Higgs couplings, the excess over the SM expectation will indicate the presence of heavy vector resonances decaying into VH and WZ final states. As we have already seen from Table 1, most of the Higgs excess comes from the 1-lepton category, while all of the ZW excess comes from the 1-lepton category but it is rather small.

The resonance search potential for a single LHC experiment and an integrated luminosity of 200 fb⁻¹, is shown in Figures 10, 11, and 12, for the 0-lepton,

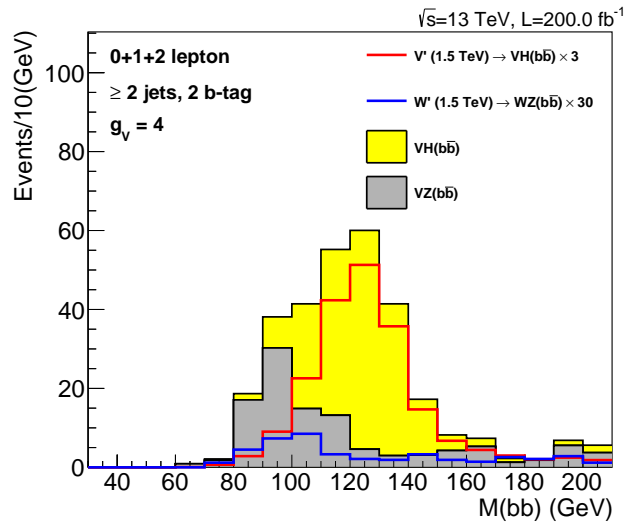


Fig. 8 Reconstructed bottom anti-bottom quark invariant mass for SM $VH \rightarrow \ell(\nu)\ell(\nu)b\bar{b}$ and $VZ \rightarrow \ell(\nu)\ell(\nu)b\bar{b}$ production (stacked yellow and gray histograms, respectively), for an integrated luminosity of 200 fb⁻¹. The HVT model predictions for $M_{V'} = 1.5$ TeV and $g_V = 4$, with VH shown in red and WH in blue, are overlaid. The plot includes all final states with 0, 1 and 2 leptons. A $p_{\perp} > 300$ GeV cut has been applied to the $b\bar{b}$ system.

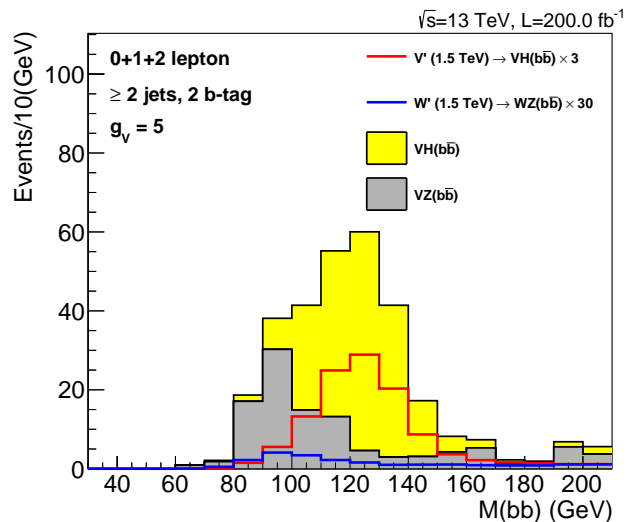


Fig. 9 Reconstructed bottom anti-bottom quark invariant mass for SM $VH \rightarrow \ell(\nu)\ell(\nu)b\bar{b}$ and $VZ \rightarrow \ell(\nu)\ell(\nu)b\bar{b}$ production (stacked yellow and gray histograms, respectively), for an integrated luminosity of 200 fb⁻¹. The HVT model predictions for $M_{V'} = 1.5$ TeV and $g_V = 5$, with VH shown in red and WH in blue, are overlaid. The plot includes all final states with 0, 1 and 2 leptons. A $p_{\perp} > 300$ GeV cut has been applied to the $b\bar{b}$ system.

1-lepton and 2-lepton categories, respectively. As seen from these results, the search is sensitive to part of the phase space not currently probed by existing searches. For 200 fb⁻¹, the sensitivity extends to masses up to about 2 TeV, and resonance widths $\Gamma/m \simeq 10\%$, al-

though the higher the width the lower the resonance mass reach. For $\Gamma/m \simeq 10\%$ only a mass up to 1.6 TeV can be reached. The reason for the search not being sensitive to larger widths is not only due to the reduction of cross section with g_V , but also due to a loss of efficiency because for V' masses greater than 1.5 GeV, the majority of b quark pairs fall in the same jet. More precisely, for resonance masses of 2 TeV or higher, the fraction of resolved $b\bar{b}$ pairs is 5% or less, respectively. Here it should be stressed that an extension of the proposed search to include fat jets could push these limits at higher values.

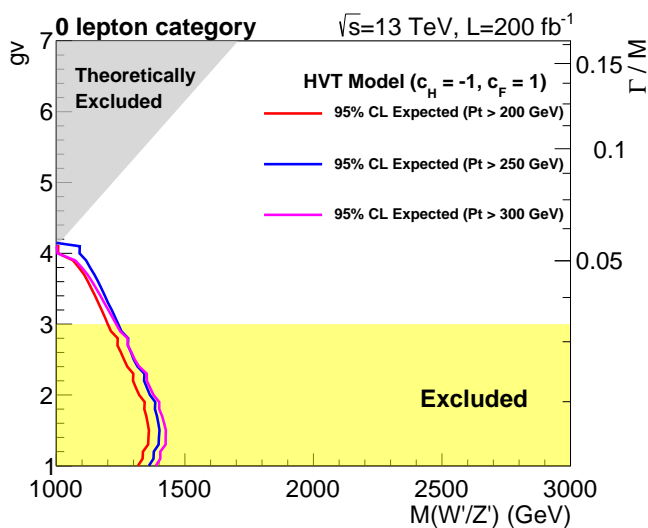


Fig. 10 Expected 95% CL HVT limits as a function of the resonance mass and width, for an integrated luminosity of 200 fb^{-1} . The limits for the 0-lepton category are shown for increasing $p_{\perp} > 200, 250, 300 \text{ GeV}$ selections. The theoretically excluded regions correspond to regions of small physical mass and large g_V coupling, where the HVT model cannot reproduce the SM input parameters α_{EW} , G_F and M_Z .

In an attempt to test the prediction of the model against the $\sim 80 \text{ fb}^{-1}$ data recently reported by ATLAS and CMS, we estimate the observed limits as shown in Figures 13, 14, and 15. The observed limits are based on the signal strength values reported by the experiments in each category. The bands corresponding to the uncertainties in the Higgs signal strength μ are not shown. The observed limits should be compared to the expected limits with $p_{\perp} > 200 \text{ GeV}$. As seen in these results, the new LHC data already exclude new parts of the allowed resonance mass-width phase space. For instance from Fig. 14, HVT resonances with $\Gamma/m = 9\%$ and mass up to 1.5 TeV, are excluded by the ATLAS experiment. The observed limits in the 1-lepton and 2-lepton categories exclude lower masses and widths than expected because of the corresponding excesses

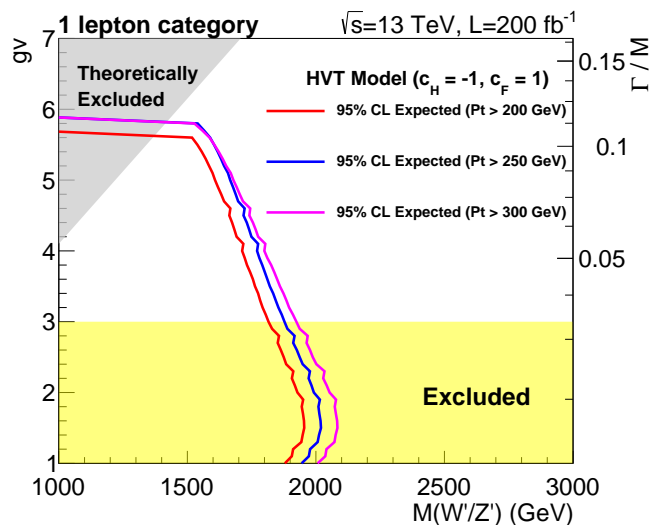


Fig. 11 Expected 95% CL HVT limits as a function of the resonance mass and width, for an integrated luminosity of 200 fb^{-1} . The limits for the 1-lepton category are shown for increasing $p_{\perp} > 200, 250, 300 \text{ GeV}$ selections. The theoretically excluded regions correspond to regions of small physical mass and large g_V coupling, where the HVT model cannot reproduce the SM input parameters α_{EW} , G_F and M_Z .

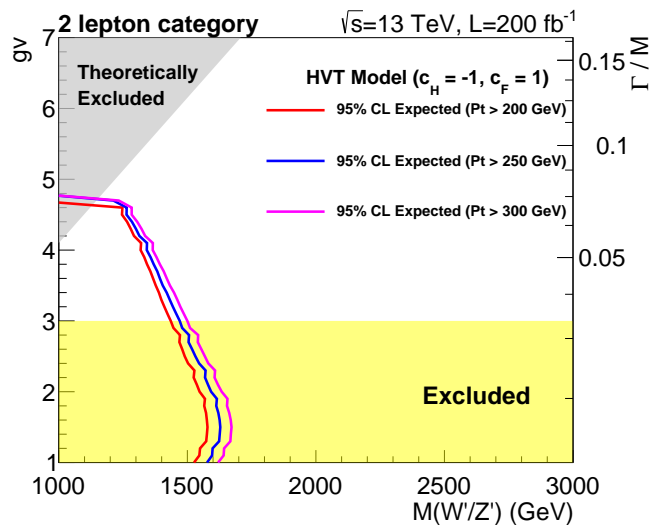


Fig. 12 Expected 95% CL HVT limits as a function of the resonance mass and width, for an integrated luminosity of 200 fb^{-1} . The limits for the 2-lepton category are shown for increasing $p_{\perp} > 200, 250, 300 \text{ GeV}$ selections. The theoretically excluded regions correspond to regions of small physical mass and large g_V coupling, where the HVT model cannot reproduce the SM input parameters α_{EW} , G_F and M_Z .

observed by the experiments. However, the uncertainties in each category are still large and more data are needed that will first settle if there is indeed an excess, and then allow to examine the compatibility of the pattern of the excess with the HVT model. It should be pointed out that the signal cross-sections were calculated at leading order, thus an additional theory uncer-

tainty due to missing higher order corrections should be considered. These theoretical uncertainties are expected to be small with respect to the rest of the systematic uncertainties of this analysis.

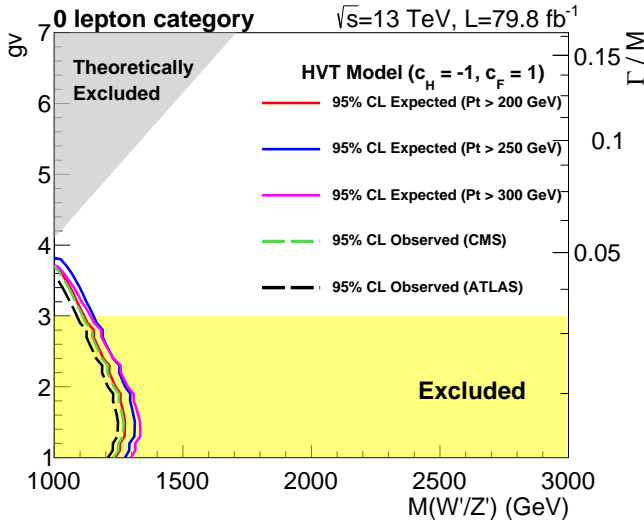


Fig. 13 Expected 95% CL HVT limits as a function of the resonance mass and width, for an integrated luminosity of 79.8 fb^{-1} . The limits for the 0-lepton category are shown for increasing $p_{\perp} > 200, 250, 300 \text{ GeV}$ selections. Estimated observed limits by ATLAS and CMS are also shown. The theoretically excluded regions correspond to regions of small physical mass and large g_V coupling, where the HVT model cannot reproduce the SM input parameters α_{EW} , G_F and M_Z .

4 Summary and Conclusions

In this work we explored the potential of a novel search of heavy vector resonances of non-zero natural width, decaying almost exclusively in the $H \rightarrow b\bar{b}$ and $Z \rightarrow b\bar{b}$ final states in association with a leptonically decaying V (Z or W) and W -only, respectively. For large g_V coupling of the exotic resonance to the W and Z bosons and the SM Higgs, the branching ratio to VH and to two gauge bosons VV dominates, leading to a simultaneous excess to both Higgs $WH \rightarrow \ell\nu b\bar{b}$, $ZH \rightarrow \ell b\bar{b}$ and non-Higgs $WZ \rightarrow \ell\nu b\bar{b}$ final states.

We showed that excesses of varying strengths should be observed in all final states (0, 1 or 2 leptons). The fact that the relative strengths of these excesses depend on branching ratios and efficiencies, provides a clear signature of the presence of heavy resonances or even their low mass tails. For a luminosity accessible by the LHC experiments of 200 fb^{-1} , the search is sensitive up to resonance masses of 2 TeV and widths Γ/m of 10%. A first test of a heavy vector triplet model against ATLAS

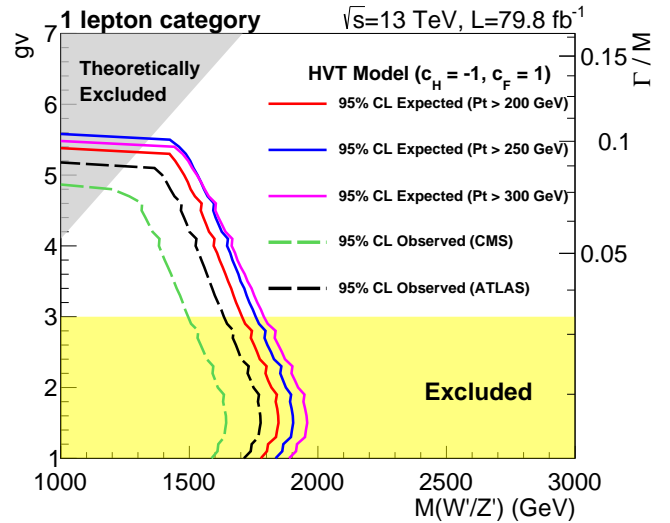


Fig. 14 Expected 95% CL HVT limits as a function of the resonance mass and width, for an integrated luminosity of 79.8 fb^{-1} . The limits for the 1-lepton category are shown for increasing $p_{\perp} > 200, 250, 300 \text{ GeV}$ selections. Estimated observed limits by ATLAS and CMS are also shown. The theoretically excluded regions correspond to regions of small physical mass and large g_V coupling, where the HVT model cannot reproduce the SM input parameters α_{EW} , G_F and M_Z .

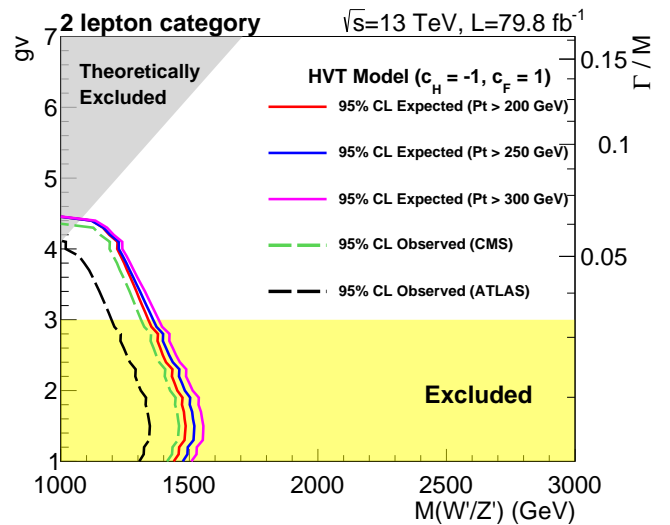


Fig. 15 Expected 95% CL HVT limits as a function of the resonance mass and width, for an integrated luminosity of 79.8 fb^{-1} . The limits for the 2-lepton category are shown for increasing $p_{\perp} > 200, 250, 300 \text{ GeV}$ selections. Estimated observed limits by ATLAS and CMS are also shown. The theoretically excluded regions correspond to regions of small physical mass and large g_V coupling, where the HVT model cannot reproduce the SM input parameters α_{EW} , G_F and M_Z .

and CMS data in terms of expected and observed limits was presented. Although experimental uncertainties on the $VH \rightarrow b\bar{b}$ signal strength μ_{VH} are still large, the LHC experiments are expected to accumulate signifi-

cant amounts of data in 2018 and beyond, making the search proposed here a very useful tool in evaluating potential excesses in Higgs yield measurements when the Higgs is produced in association with a weak vector boson.

Acknowledgements

This work was supported by the Taiwanese Ministry of Science and Technology under grant number 106-2112-M-002-011-MY3.

References

1. J. C. Pati and A. Salam, Lepton Number as the Fourth Color, *Phys. Rev. D* 10 (1974) 275.
2. H. Georgi and S. Glashow, Unity of All Elementary Particle Forces, *Phys. Rev. Lett.* 32 (1974) 438.
3. H. Fritzsch and P. Minkowski, Unified Interactions of Leptons and Hadrons, *Annals Phys.* 93 (1975) 193.
4. E. Eichten and K. Lane, Low-Scale technicolor at the Tevatron and LHC, *Phys. Lett. B* 669 (2008) 235.
5. R. Contino, The Higgs as a Composite Nambu-Goldstone Boson, arXiv:1005.4269 [hep-ph] (2010).
6. T. Han, H. E. Logan, B. McElrath, and L.-T. Wang, Phenomenology of the little Higgs model, *Phys. Rev. D* 67 (2003) 095004.
7. M. Schmaltz and D. Tucker-Smith, Little Higgs Theories, *Ann. Rev. Nucl. Part. Sci.* 55 (2005) 229.
8. M. Perelstein, Little Higgs models and their phenomenology, *Prog. Part. Nucl. Phys.* 58 (2007) 247.
9. V. D. Barger, W.-Y. Keung, and E. Ma, A gauge model with light W and Z bosons, *Phys. Rev. D* 22 (1980) 727.
10. E. Salvioni, G. Villadoro, and F. Zwirner, Minimal Z' models: present bounds and early LHC reach, *JHEP* 09 (2009) 068.
11. C. Grojean, E. Salvioni, and R. Torre, A weakly constrained W' at the early LHC, *JHEP* 07 (2011) 002.
12. ATLAS Collaboration, Search for diboson resonances with boson-tagged jets in pp collisions at $\sqrt{s} = 13$ TeV with the ATLAS detector, *Phys. Lett. B* 777 (2017) 91.
13. ATLAS Collaboration, Searches for heavy ZZ and ZW resonances in the $\ell\ell q\bar{q}$ and $\nu\nu q\bar{q}$ final states in pp collisions at $\sqrt{s} = 13$ TeV with the ATLAS detector, arXiv:1708.09638 [hep-ex] (2017).
14. ATLAS Collaboration, Search for WW/WZ resonance production in $\ell\nu q\bar{q}$ final states in pp collisions at $\sqrt{s} = 13$ TeV with the ATLAS detector, arXiv:1710.07235 [hep-ex] (2017).
15. ATLAS Collaboration, Search for heavy resonances decaying into a W or Z boson and a Higgs boson in final states with leptons and b-jets in 36 fb^{-1} of $\sqrt{s} = 13$ TeV pp collisions with the ATLAS detector, arXiv:1712.06518 [hep-ex] (2017).
16. ATLAS Collaboration, Search for heavy resonances decaying into a W or Z boson and a Higgs boson in the $qqbb$ final states in pp collisions at $\sqrt{s} = 13$ TeV with the ATLAS detector, *Phys. Lett. B* 774 (2017) 494.
17. CMS Collaboration, Search for heavy resonances decaying into a vector boson and a Higgs boson in final states with charged leptons, neutrinos and b quarks at $\sqrt{s} = 13$ TeV, arXiv:1807.02826 [hep-ex] (2018).
18. CMS Collaboration, Search for new heavy resonances decaying into a Z boson and a massive vector boson in the $2\ell 2q$ final state at $\sqrt{s} = 13$ TeV, CMS-PAS-B2G-17-013 (2017).
19. CMS Collaboration, Search for heavy resonances decaying to pairs of vector bosons in the $\ell\nu q\bar{q}$ final state at $\sqrt{s} = 13$ TeV, CMS-PAS-B2G-16-029 (2017).
20. CMS Collaboration, Search for heavy resonances decaying into a Z boson and a vector boson in the $\nu\nu q\bar{q}$ final state, CMS-PAS-B2G-17-005 (2017).
21. CMS Collaboration, Search for heavy resonances that decay into a vector boson and a Higgs boson in hadronic final states at $\sqrt{s} = 13$ TeV, *Eur. Phys. J. C* 77 (2017) 9, 636.
22. CMS Collaboration, Combination of searches for heavy resonances decaying to WW , WZ , ZZ , WH , and ZH boson pairs in proton proton collisions at $\sqrt{s} = 8$ and 13 TeV, *Phys. Lett. B* 774, 533 (2017).
23. ATLAS Collaboration, Combination of searches for heavy resonances decaying into bosonic and leptonic final states using 36 fb^{-1} of proton proton collision data at $\sqrt{s} = 13$ TeV with the ATLAS detector, *Phys. Rev. D* 98 (2018) 5.
24. M. Hoffmann, A. Kaminska, R. Nicolaidou, S. Paganis, Probing Compositeness with Higgs Boson Decays at the LHC, *Eur. Phys. J. C* 74 (2014) 11, 3181.
25. D. Pappadopulo, A. Thamm, R. Torre and A. Wulzer, Heavy Vector Triplets: Bridging Theory and Data, *JHEP* 09 (2014) 060.
26. ATLAS Collaboration, Observation of $H \rightarrow b\bar{b}$ decays and VH production with the ATLAS detector, arXiv:1808.08238 [hep-ex] (2018).
27. CMS Collaboration, Observation of Higgs boson decay to bottom quarks CMS-PAS-HIG-18-016 (2018).
28. J. Alwall et. al. Madgraph 5 : Going beyond, arXiv:1106.0522v1 [hep-ph] (2011).
29. T. Sjostrand, S. Mrenna, P. Skands, A Brief Introduction to PYTHIA 8.1, *Comput. Phys. Commun.* 178 (2008) 852.
30. S. Ovnyn, X. Roubly, V. Lemaitre, DELPHES, a framework for fast simulation of a generic collider experiment, arXiv:0903.2225 [hep-ph] (2009).
31. G. Cowan, K. Cranmer, E. Gross, O. Vitells, Asymptotic formulae for likelihood-based tests of new physics, *Eur. Phys. J. C* 71 (2011) 1 – 19.